Design and Development of 3-DOF Modular Micro Parallel Kinematic Manipulator

C.C. Ng†, S.K. Ong* and A.Y.C. Nee*†
†Singapore-MIT Alliance
*Mechanical Engineering Department, Faculty of Engineering
National University of Singapore, 9 Engineering Drive 1, Singapore 117576

This paper presents the research and development of a 3-legged micro Parallel Kinematic Manipulator (PKM) for positioning in micro-machining and assembly operations. The structural characteristics associated with parallel manipulators are evaluated and PKMs with translational and rotational movements are identified. Based on these results, a hybrid 3-UPU (Universal Joint-Prismatic Joint-Universal Joint) parallel manipulator is designed and fabricated. Kinematic algorithm and workspace visualization are presented for this hybrid 3-UPU manipulator. The principles of the operation and modeling of this micro PKM is largely similar to a normal size Stewart Platform (SP). A modular design methodology is introduced for the construction of this micro PKM. Calibration results of this hybrid 3-UPU PKM are discussed in this paper.

Keywords: Micro parallel kinematic manipulator, modular design, Stewart Platform, workspace simulation.

I. Introduction

The recent trends towards high speed machining due to the demand for higher accuracy and greater dexterity have motivated the research and development of new novel types of parallel kinematics machines [1]. A parallel manipulator is a closed-loop mechanism where a moving platform is connected to the base by at least two serial kinematics chains (legs). The conventional Stewart Platform (SP) manipulator has six extensible legs and hence a very rigid kinematics structure [2]. Compared to serial kinematics manipulators, an SP has the desirable characteristics of high payload and rigidity. However, the drawback of an SP is a much limited working envelope, more complex direct kinematics and control algorithms, coupled problems of the position and orientation movements, as well as the precise spherical joints are difficult to manufacture at low cost [3].

A new trend in the development of Parallel Kinematics Manipulators (PKM) is the reduction from six DOFs to three. The decrease of DOFs of the PKM has advantages in workspace and cost reduction. However, a 3-DOF PKM provides less rigidity and DOFs. To overcome these shortcomings, PKMs with fewer than six DOFs have been actively investigated. Clavel [4] and Sternheim [5] reported a 4-DOF high speed robot called the Delta Robot. Lee and Shah [6] analyzed a 3-DOF parallel manipulator. Some 3-DOF parallel manipulator architectures provide pure relative rotation of the mobile platform about a fixed point and are used as pointing devices, wrists of manipulators and orienting devices [7, 8]. Furthermore, Tsai [9] introduced a novel 3-DOF translational platform that is made up of only revolute joints. It performs pure translational motion and has a closed-form solution for the direct and inverse kinematics.

In addition, a purely 3-DOF translational or rotational motion would require the activation of all the six legs, which means an increase in energy consumption [10]. Hence, in terms of cost and complexity, a 3-DOF 3-legged micro PKM is cost effective and the kinematics of the mechanism is further simplified for the purpose of control.

To increase the flexibility and functionality of the micro PKM developed in this research, the concept of modular design has been introduced. In recent years, modular robots have increasingly been proposed as a means to develop reconfigurable and self-repairable robotic systems [11]. Modular robots consisting of many autonomous units or modules can be reconfigured into a large number of designs. Based on the modular design concept, three PKMs have been configured virtually for this research using a solid modeling system and the same modular components as shown in Fig. 1. In Fig. 1, platforms with only rotational movements, translational movements, as well as a hybrid UPU platform can be assembled by interchanging the spherical and the universal joints or adding extra rigid links.

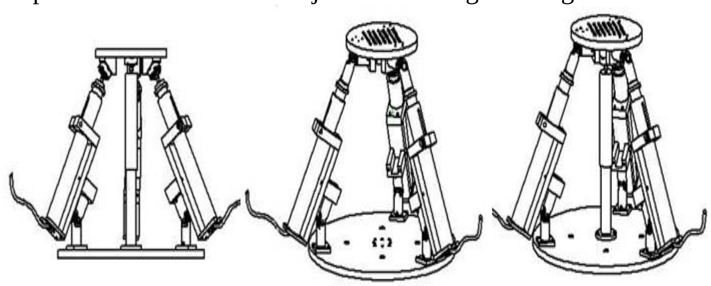

Fig. 1 Parallel manipulator systems fabricated using the same modular components.

Ideally, the modules should be uniform and self-contained. These modules must interact with one another and co-operate to realize self-configuration. The robot can change from one configuration to another manually or automatically. Hence, a modular manipulator can be reconfigured or modified to adapt to a new environment. In addition, a modular micro PKM can have self-repairing capability by removing and replacing failed modules. Since self-reconfigurable modular robots can provide the functionality of many traditional mechanisms, they are especially suited for a variety of tasks, such as high speed machining [1] in the precision engineering industry.

II. BACKGROUND

In this research, the objectives of the development of the micro PKM, i.e., Micro Parallel Kinematic Manipulator (MSP) are the minimization of the dimensions of the system and the portability of the system, e.g., portable on a CNC machine. For the minimization of the dimensions of the MSP, the number of links of the platform is reduced from six to three. The DOF for a closed-loop PKM is examined using the Grübler's formula:

$$F_e = \lambda(l - j - 1) + \sum_{i=1}^{j} f_i - I_d \qquad (1)$$

where F_e is the effective DOF of the assembly or mechanism, λ is the DOF of the space in which the mechanism operates, l is the number of links, j is the number of joints, f_i is the DOF of the i-th joint, and I_d is the idle or passive DOFs.

The number of joints is nine (six universal joints and three prismatic joints). The number of links is eight (two links for each actuator, the end effectors and the base). The sum of all the DOFs of the joints is 15. Hence, using Grübler's formula, the DOF of the micro PKM is computed as $F = 6(8-9-1)+15 = 3$. Using a systematic enumeration methodology developed by Tsai [14], a comparison study of the configurations is performed to select a configuration that meets the requirement of the parallel kinematics system to be constructed in this research.

Therefore, various designs of PKMs are simulated on a micro scale using Matlab, such as a 6-legged SP, 3-legged PKM and 6-legged PUS SP, where PUS denotes a platform with links of prismatic joint, universal joint and spherical joint. The workspace of these platforms are simulated as shown in Fig.2, and compared to select the most suitable design to achieve the research objectives.

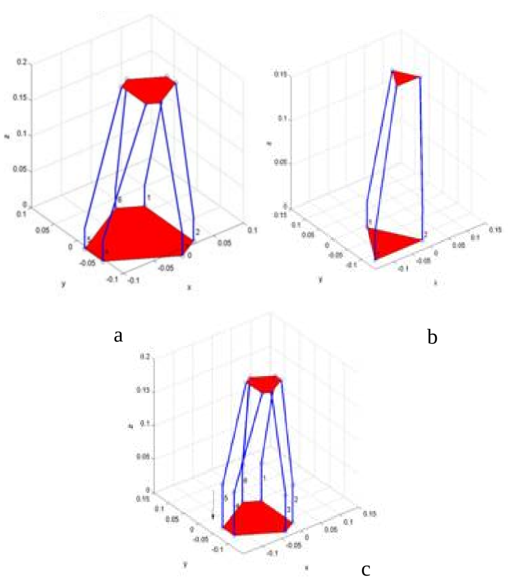

Fig. 2(a) 6-legged micro Stewart Platform, (b) 3-legged micro Stewart Platform, and (c) PSU micro Stewart Platform.

III. MATHEMATICAL MODEL

To analyze the kinematics model of the parallel mechanism, two relative coordinate frames are assigned, as shown in Fig. 3. A static Cartesian coordinate frame $X_BY_BZ_B$ is fixed at the center of the base while a mobile Cartesian coordinate frame $X_PY_PZ_P$ is assigned to the center of the mobile platform. P_i, i = 1, 2, 3 and B_i, i = 1, 2, 3 are the joints that are located at the center of the base and the platform passive joints respectively. A passive middle link L_m is installed at the middle of the platform to constrain the kinematics of the platform to perform translation along the Z-axis and rotational around the X- and Y-axes.

Let r_B and r_P be the radii of the base and the platform passing though joints P_i and B_i (i = 1, 2, 3), respectively. The position of B_i with reference to the fixed coordinate frame $X_BY_BZ_B$ can be expressed in equation (2).

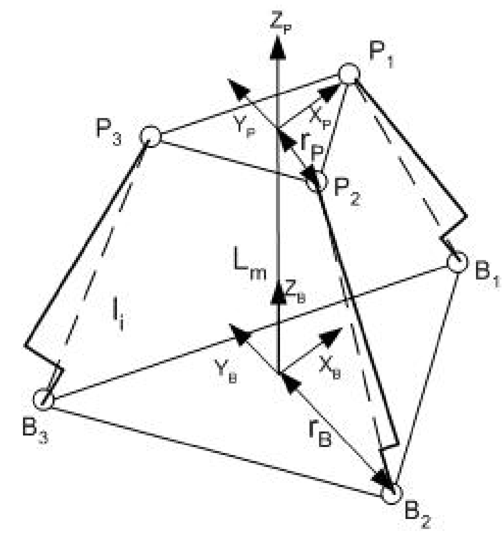

Fig. 3 Schematic diagram of the PKM.

$$B_1 = \begin{bmatrix} r_B & 0 & 0 \end{bmatrix}^T \qquad B_2 = \begin{bmatrix} -\frac{1}{2} r_B & \frac{\sqrt{3}}{2} r_B & 0 \end{bmatrix}^T$$

$$B_3 = \begin{bmatrix} -\frac{1}{2} r_B & -\frac{\sqrt{3}}{2} r_B & 0 \end{bmatrix}^T \qquad (2)$$

The positions of joints P_i, (i = 1, 2, 3) are expressed with respect to the mobile frame $X_PY_PZ_P$ in equation (3).

$$P_1 = \begin{bmatrix} r_P & 0 & 0 \end{bmatrix}^T \qquad P_2 = \begin{bmatrix} -\frac{1}{2} r_P & \frac{\sqrt{3}}{2} r_P & 0 \end{bmatrix}^T$$

$$P_3 = \begin{bmatrix} -\frac{1}{2} r_P & -\frac{\sqrt{3}}{2} r_P & 0 \end{bmatrix}^T \qquad (3)$$

Since the proposed MSP is to be built within a limited space of 300mm × 300mm × 300mm, the actuators with length of 216mm are too long to be assembled directly onto the base joints. Instead of assembling the actuators on top of the joints, the actuators are aligned parallel to the joints as shown in Fig. 4. Therefore, the calculation of the length of the link is not as direct as the inverse kinematics of a normal

SP. As shown in Fig. 5, the length of the link can be calculated using equation (4).

$$\vec{l}_i = -\vec{B}_i + \vec{t} + \underline{R} \cdot \vec{P}_i \text{ , i = 1 ... 3} \qquad (4)$$

where l_i is the dotted link length, and $\vec{t}$ and R are the translation and orientation of P_i with respect to $[X_P\ Y_P\ Z_P]^T$. However, for this present hybrid PKM, extra calculation steps in equations (5)-(8) are needed as shown in Fig. 4.

$$x^2 + a^2 = y^2 \qquad (5)$$

$$\frac{k-x}{x} = \frac{z}{a} = \frac{L-y}{y} \Rightarrow y = \frac{xL}{k} \qquad (6)$$

$$x = \sqrt{\frac{a^2}{(\frac{L^2}{k^2}) - 1}} \qquad (7)$$

$$z = a \times \frac{k-x}{x} = \left(\frac{k - \sqrt{\frac{a^2}{\frac{L^2}{k^2} - 1}}}{\sqrt{\frac{a^2}{\frac{L^2}{k^2} - 1}}} \right) \times a \qquad (8)$$

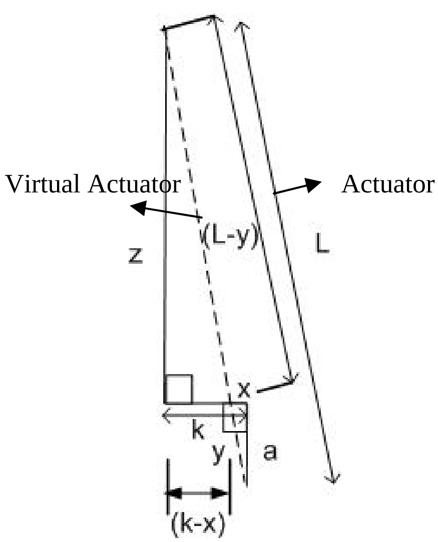

Fig. 4 Calculation of the actual stroke of the link.

By determining the length of the dotted link, L_i using inverse kinematics, the length of Z can be determined using the similarity triangular theory as shown in equation (8). Hence, the strokes of the links can be found indirectly based on the manipulation of the platform. After analyzing the stroke through inverse kinematics methods, the required rotational angle of the base joints and platform joints can be further affirmed through determining the angles of rotation as shown in Fig. 5.

The geometry matrix method of analysis was used since for parallel manipulators, it is often more convenient to employ the geometric method [12]. Generally, a vector-loop equation is written for each limb, and the passive joint variables are eliminated among these equations as shown in Fig. 5.

Let $X = \alpha, Y = \beta, Z = \sigma$ and L_i+H = M_i, since L_i is known from the similarity triangle equation. Furthermore, Z_i (i = 1, 2, 3) is known based on the coordination of each base joints, which are 0°, 120° and 240°. Besides, $B_i = \begin{bmatrix} r_{xi} & r_{yi} & 0 \end{bmatrix}^T$, i = 1, 2, 3 is also known from equation (3). Based on inverse kinematics of the platform, one can determine the point $\begin{bmatrix} P_{x_i} \\ P_{y_i} \\ P_{z_i} \end{bmatrix}$, i = 1, 2, 3 from equation (4).

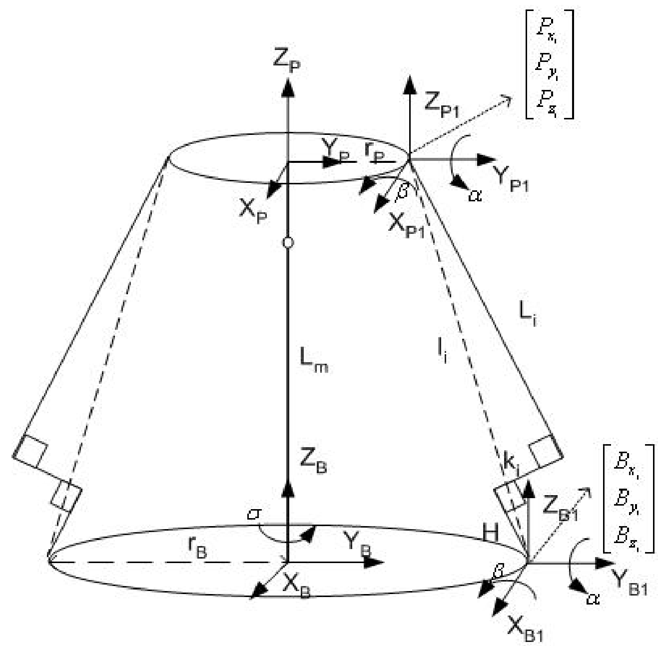

Fig. 5 Geometry method diagram.

Thus, for a known platform position, one can calculate the rotation angles, X_i and Y_i based on the known actuator stroke length using equation (9).

$$\therefore R_z \times R_{xy} \times \begin{bmatrix} 0 \\ k_i \\ Mi \end{bmatrix} + \begin{bmatrix} r_{xi} \\ r_{yi} \\ 0 \end{bmatrix} = \begin{bmatrix} P_{x_i} \\ P_{y_i} \\ P_{z_i} \end{bmatrix} \qquad (9)$$

where,

$$R_z = \begin{bmatrix} \cos Z_i & -\sin Z_i & 0 \\ \sin Z_i & \cos Z_i & 0 \\ 0 & 0 & 1 \end{bmatrix} \text{ and } R_{XY} = \begin{bmatrix} \cos Y_i & \sin Y_i \sin X_i & \sin Y_i \cos X_i \\ 0 & \cos X_i & -\sin X_i \\ -\sin Y_i & \cos Y_i \sin X_i & \cos Y_i \cos X_i \end{bmatrix}.$$

Hence, through elaboration of equation (9), the solutions for the rotation angle X_i, Y_i where i = 1, 2, 3 can be found. Hence, through determining the rotation angle of each universal joint of the links, the stroke of the actuators can be determined. The known rotation angle is also used as a geometry constraint to determine the workspace of the platform. After the determination of the stroke and angle of rotation of all the universal joints of the actuators, a simulated hybrid 3-UPU PKM can be plotted using Matlab as shown in Fig. 6. A passive middle link is installed and attached via a spherical joint to the platform as shown Fig. 7. The passive middle link acts as a constraint for the extra DOF of the platform. The inverse and forward kinematics algorithms of this hybrid PKM are implemented using Matlab, and the movement of the platform is simulated to verify the mobility of the platform.

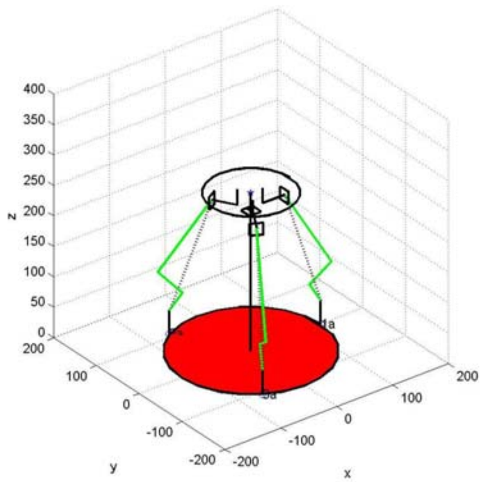

Fig. 6 Modified SP with a passive prismatic middle link.

IV. Optimization method and analysis of workspace

Based on the inverse and forward kinematics algorithms of the platform, and due to the fact that all legs are equal and the distance between the joints at the base and platform are equilateral, the workspace of the hybrid 3-UPU platform depends on three geometric parameters, namely, (a) the stroke of the prismatic link, L_i, (b) the limitation of the universal joints angle of the base and platform, which is 45° and (c) the distances K between the spherical joint of the middle link to the middle point of the moving platform as shown in Fig. 7.

The stroke L_i of the actuator is the travel range of each prismatic link, which is 50mm. As shown in Fig. 8, the workspace describes the manipulation of point **P**, which is at the middle of the mobile platform, with respect to the middle point **B** of the base, as shown in Fig. 5. For each orientation of the platform, the middle point **P** is rotated with respect to point **S** at the center of the spherical joint, which is located at the middle link of the platform as shown in Fig. 7.

During the optimization process, each position of the point **P** at the mobile platform is verified with its geometry constraints for every manipulation of the platform. The lengths of the legs are determined using inverse kinematics, i.e., equation (8). Next, the lengths of the legs are checked to determine if they are within the allowable interval $L_{min}<L_i<L_{max}$ and the interference of the legs is also checked. In addition, for rotation movements of the platform, the joint angles are determined and verified. After all the geometry constraints have been verified, the verified Cartesian coordinates of point **P** are recorded in the workspace database.

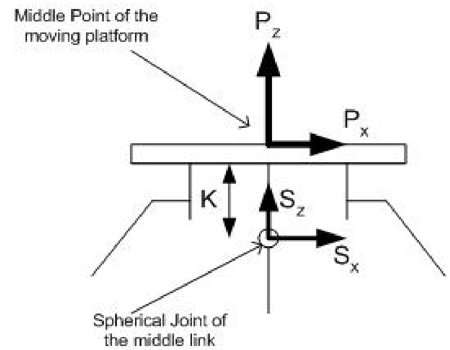

Fig. 7 Relationship between the point P and the spherical joint S.

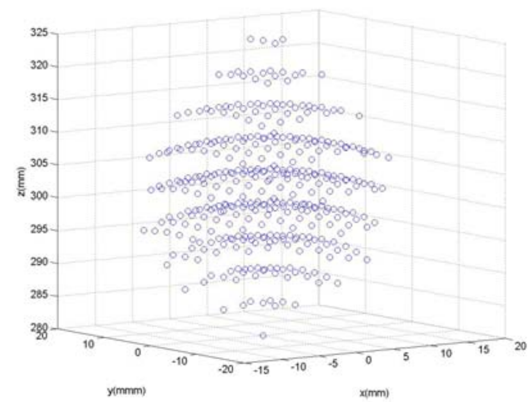

Fig. 8 Workspace of the surface point of the hybrid PKM.

The workspace optimization program is implemented using Matlab. The workspace data points collected using the optimization program are plotted using Matlab as shown in Fig. 8, which also shows the workspace of the optimal constrained configuration. The points represent the position that can be achieved by point **P** of the mobile platform. The workspace of point **P** describes a portion of a sphere with its center at point **S** and a radius **K**. The workspace volume of point **P** increases gradually during the incremental motion of point **P** along Z-axis. The workspace volume increases to its maximum when the platform is located at Z = 310mm. Overall, the workspace forms a diamond shape. The volume of the workspace is 93875mm^3, which is relatively small as compared with other modular PKM configurations. However, the objective of this hybrid micro PKM is for fine machining movements along the Z-axis as well as rotational movements around the X- and Y-axes. Hence, the simulated workspace shows that the platform is constrained from over traveling. Although this system has a limited Cartesian workspace, in term of angular workspace, it can rotate up to 32° around the X-axis and 28.2° around the Y-axis when the Z position is 310mm. Furthermore, the platform can travel 450mm along the Z-axis. From the results of the workspace analysis, the workspace is affected significantly by the limitation of the stroke of the actuators and the imposed angle of the universal joints.

V. Design of the Micro Paralell Manipulator

A set of design criteria that has been formulated based on the literature review of PKMs and the results of the workspace analysis is applied in the fabrication and design of the hybrid 3-UPU PKM. To shorten the development cycle [2], the modular design methodology is employed in the prototype development.

Based on the research reported by Dash et al [15], a modular parallel robot may have an unlimited number of configurations depending on the inventory of the modules. Principally, the modules for assembly into a modular micro PKM can be divided into two groups:

a) Fixed Dimension Modules

This group includes actuator modules, passive joint modules (rotary, pivot and spherical joints) and end-effector joints, such as the PI M-235.5DG actuators, Hephaist spherical joints and Miniature Acetal Fork Type Universal Joints.

Fig. 9 The PI M-235.5DG actuator, Universal Joint and Spherical Joint.

b) Variable Dimension Modules

This group provides the end-users with the ability to rapidly fine-tune the kinematic and dynamic performance of the manipulators, and consists of rigid links, joints connectors and platform modules, as shown in Fig. 10. They can be rapidly assembled into various layouts with different kinematic and dynamic characteristics.

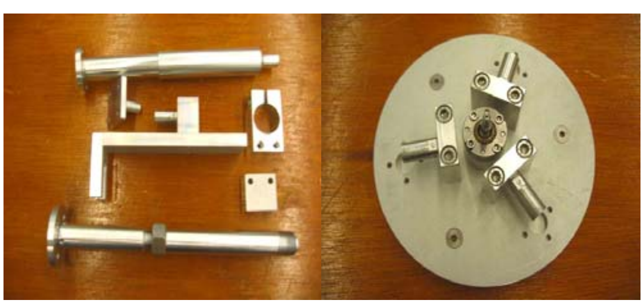

Fig. 10 The connectors, Links and the mobile platform.

VI. Prototype Development

Therefore, based on these concepts, three PKM prototypes have been developed and assembled to compare their characteristics and functions in an actual working environment.

To maintain a high rigidity of the platforms, the DOFs of these systems can be constrained through the installation of extra joints or the reduction of the DOF of the joints. For the 4-legged platform in Fig. 11(a), a fixed rigid link with a spherical joint is installed in the middle of the platform so that the motion of the platform is limited to angular rotation only. Thus, it can perform pure rotational movements. For the system in Fig. 11(b), the spherical joints of the platform have been replaced with universal joints. Hence, this platform is limited to translational movements through the axes of the universal joints. Another 3-DOF PKM is configured as shown in Fig. 12. It is a hybrid 3-DOF platform that consists of translation movements along the Z-axis and rotation movements around the X- and Y-axes.

Furthermore, due to the introduction of the modular design concept through fabricating interchangeable parts, the 3-DOF PKM can be easily modified from a translational platform to a rotational platform. An extra link or active joints can be introduced in future to increase the DOF of the micro PKM.

Fig. 11 (a) Pure translational platform, and (b) pure rotational platform.

Calibrations and various tests have been performed on the modular PKMs. Architectural singularities [16] have been detected during the calibration of the pure translational PKM while it is in the static position. It is found that in a static position, extra DOFs are introduced as some geometry conditions are not met, such as all the revolute pair axes at the ends of the links do not converge towards a single point, and each link has two intermediate resolute pair axes that are not parallel to one another and perpendicular to the straight line through the centre of the universal joint [17]. Hence, a careful assembly of the modular units of the platform satisfying certain geometry conditions is needed to attain a controllable pure translational motion.

Since all the links are composed of 2-DOF universal joints, prismatic links and 3-DOF spherical joints, by installing a fixed link with a spherical joint at the centre of the platform, the motion of the platform is limited to purely rotational movements around a fixed point. The major disadvantage of this type of configuration is that the platform cannot perform Z-axis movements, which is a crucial requirement for micro-machining. The over-constrained design of this platform with a fixed middle link causes a high risk of damage to the platform when it is manipulated outside the defined workspace.

Fig. 12 Hybrid 3-UPU PKM.

Hence, a hybrid PKM has been assembled by installing a passive prismatic link at the centre of the pure translational platform as shown in Fig. 12, and the singularity problem is solved. By installing a passive prismatic link in the middle of the platform and attached to the platform by a spherical joint, the extra DOF caused by the universal joints of the links is constrained. Thus, the hybrid PKM is able to perform movements along the Z-axis and rotation about the X- and Y-axes. Among the three PKMs architectures that have been configured, the hybrid platform is further elaborated as it can be coupled with the present normal-sized SP to perform as a micro manipulator for a tool holder to perform machining operations on a workpiece that is fixtured on the SP.

VII. Error Calibration USING CMM

After the development of the simulation and interfacing programs, error calibration was performed using a CMM machine. The accuracy and repeatability of the platform was determined to be 100 micron. The setup of the micro PKM on the CMM machine is shown in Fig. 13.

The calibration was performed by manipulating the platform to the theoretical positions and orientations using a visual C++ interface. Next, the data of the coordinates from the surface of the platform was collected to determine the actual surface plane of the platform. Using the CMM machine, the measurement variations between the actual and theoretical angles and positions were compared. The results of the calibration are shown in Table 1.

From Fig. 14, the maximum error of the roll angle is 1.171°, the maximum error of the pitch angle is 2.1461°, and the maximum error of the Z-axis displacement is -3.249mm. At least two errors occurred in the same data set when the platform was translating and rotating simultaneously within the allowable maximum rotation angles. However, when the platform was performing purely translation movements, the error of the displacement is within ±0.42mm.

The variations of the angular rotation and the translation movement of the Z-axis are acceptable. The overall average errors of the angular rotation and translation are 0.063942° for the roll rotation, 0.186244° for the pitch rotation, and 0.42854mm for the Z-axis movement. From the calibration results, the errors of the rotational angle and position increase when the platform has reached the maximum rotational angle, which is the boundary of the calculated workspace.

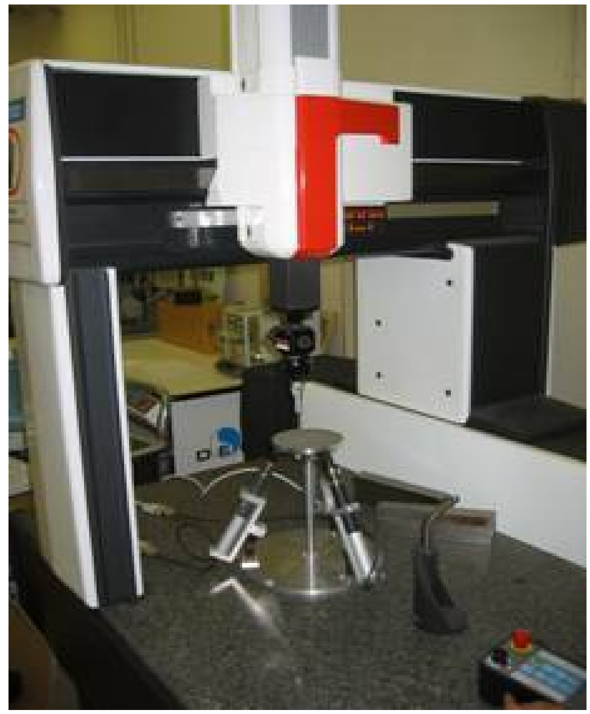

Fig. 13 Calibration of micro PKM using CMM.

VIII. Conclusion

This paper addresses the kinematics analysis of the hybrid PKM that has been designed and developed in this research to perform translation along the Z-axis and rotation about the X- and Y-axes. Modular configurations of the various PKMs are successfully assembled using the same modular units. An algorithm for the optimal design of the hybrid PKM has been presented. In particular, the proposed formulation represents an integration of the relevant aspects of the dimensional design of parallel manipulators in a multi-objective optimization design using workspace characteristics. A 3-DOF PKM has been constructed which inverse kinematics can be solved analytically. The developed inverse kinematics algorithm of the PKMs can be used for similar modular platform configurations through using different constraint settings. This algorithm has been successfully implemented to control the hybrid PKM. The hybrid micro PKM that has been developed is calibrated based on the simulated workspace. The errors are within 0.2° and 0.5mm. In conclusion, the platform is able to travel to the required position and orientation smoothly and accurately for the precision engineering industry.

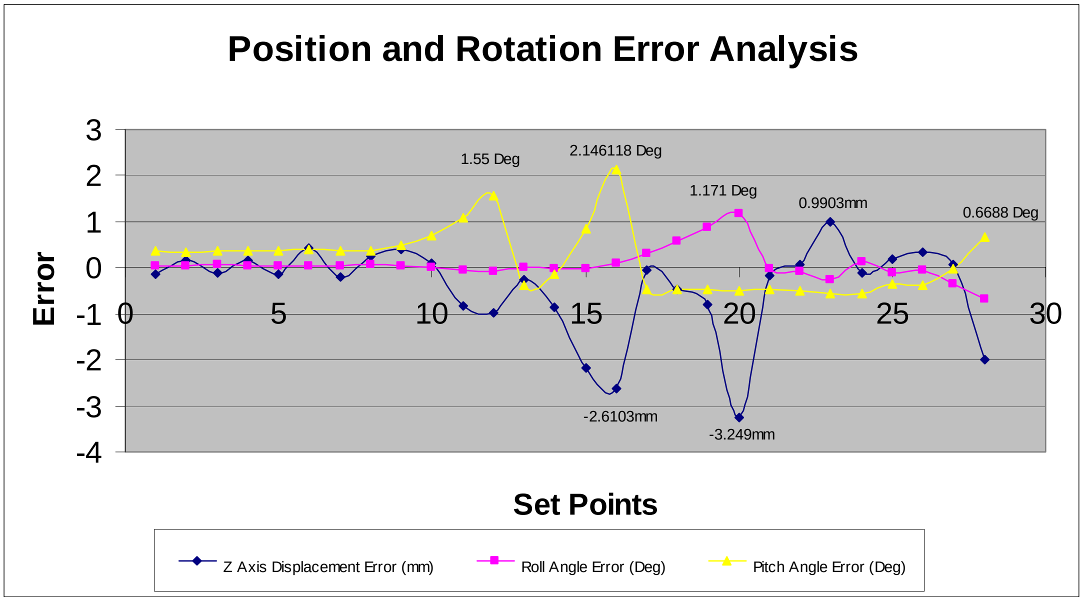

Fig. 14 Displacement and rotational error.

Table 1. Calibration result of the micro SP

Theoretical Position and Orientation			Actual Position and Orientation			Position and Orientation Error		
Rotation X°	Rotation Y°	Position Z (mm)	Z (mm)	Actual X°	Actual Y°	Z error (mm)	Angle X error°	Angle Y error°
0	0	279	278.8502	-0.0452256	-0.365286	-0.1498	0.045225568	0.365286
0	0	304	304.157	-0.0397824	-0.372792	0.157	0.039782411	0.372792
0	0	328	328.4152	-0.0470018	-0.395424	0.4152	0.047001757	0.395424
0	0	314	314.2583	-0.0551378	-0.382016	0.2583	0.055137845	0.382016
5	0	314	314.4069	4.9566289	-0.478564	0.4069	0.043371086	0.478564
10	0	314	314.1093	10.005325	-0.708506	0.1093	-0.0053253	0.708506
15	0	314	313.1804	15.051127	-1.091752	-0.8196	-0.05112695	1.091752
20	0	310	309.0273	20.087883	-1.563315	-0.9727	-0.08788319	1.563315
-5	0	310	309.7469	-5.0196374	0.3754471	-0.2531	0.019637435	-0.37545
-10	0	310	309.1461	-10.025349	-0.128134	-0.8539	-0.02535	-0.12813
-15	0	310	307.8201	-15.026953	0.8498897	-2.1799	-0.02695	0.84989
-20	0	310	307.3897	-19.908848	2.1461184	-2.6103	0.091152	2.146118
0	5	310	309.9521	0.3101281	4.5267511	-0.0479	0.310128	-0.47325
0	10	310	309.5268	0.5645316	9.5351477	-0.4732	0.564532	-0.46485
0	15	310	309.1953	0.8663929	14.535792	-0.8047	0.866393	-0.46421
0	20	310	306.751	1.1710863	19.495447	-3.249	1.171086	-0.50455
0	-5	310	309.8145	-0.0267188	-5.48063	-0.1855	-0.02672	-0.48063
0	-10	310	310.0537	-0.0847028	-10.51162	0.0537	-0.0847	-0.51162
0	-15	310	310.9903	-0.25665	-15.54496	0.9903	-0.25665	-0.54496
5	5	310	309.9001	5.1334433	4.4381289	-0.0999	0.133443	-0.56187
10	10	310	310.2003	9.8857264	9.6356161	0.2003	-0.11427	-0.36438
-5	-5	310	310.3308	-5.0607633	-5.386758	0.3308	-0.06076	-0.38676
-10	-10	310	310.0731	-10.365204	-10.03466	0.0731	-0.3652	-0.03466
-15	-15	310	308.0145	-15.678278	-14.33112	-1.9855	-0.67828	0.668877

=Maximum Error

REFERENCES

[1] S.A. Joshi, L.W. Tsai, 2003, “The Kinematics of a Class of 3-DOF, 4-Legged Parallel Manipulators”, Transactions of the ASME, Vol. 125, pp. 52-60.

[2] G. Yang, I.M. Chen, W.H. Chen, S.H. Yeo, 2003, “Design and Analysis of a 3-RPRS Modular Parallel Manipulator for Rapid Deployment,” Proceedings of the IEEE/ASME International Conference on Advanced Intelligent Mechatronics, Kobe, Japan, pp. 1250-1255.

[3] L.W. Tsai, G.C. Walsh, R.E. Stamper, 1996, “Kinematics of a Novel Three DOF Translational Platform”, Proceedings of the 1996 IEEE International Conference on Robotics and Automation Minneapolis, Minnesota – April 1996, pp. 3446-3451.

[4] R. Clavel, 1988, “DELTA, A Fast Robot with Parallel Geometry,” Proceedings of the 18th International Symposium on Industrial Robots, pp. 91-100.

[5] F. Sternheim, 1987, ‘Computation of the Direct and Inverse Kinematics Model of the Delta 4 Parallel Robot,” Robotersysteme, Vol. 3, pp. 199-203.

[6] K. Lee, D.K. Shah, 1987, “Kinematic Analysis of a Three Degrees of Freedom In-Parallel Actuated Manipulator”, Proceedings of the IEEE International Conference On Robotics and Automation, pp. 345-350.

[7] H. Asada, J.A. Cro Granito, 1985, “Kinematic and Static Characterization of Wrist Joints and Their Optimal Design” Proceedings of IEEE International Conference on Robotics and Automation, St. Louis, pp. 91-100.

[8] C. Gosselin, J. Hamel, 1994, “The Agile Eye: Agile Performance Three-Degree-of Freedom Camera-Orienting Device,” Proceedings of the IEEE International Conference on Robotics and Automation, pp. 781-786.

[9] L.W. Tsai, G.C. Walsh, R. Stamper, 1996, “Kinematics of a Novel Three DOF Translational Platform,” Proceedings of the 1996 IEEE International Conference on Robotics and Automation, Minneapolis, MN, pp. 3446-3451.

[10] M. Badescu, C. Mavroidis, J. Morman, 2002, “Workspace Optimization of Orientational 3-Legged UPS Parallel Platforms”, Proceedings of the 2002 ASME International Design Engineering Technical Conferences and the Computers and Information in Engineering Conference (DETC/CIE), Montreal, Canada, September 2002, DETC2002/MECH-34366. pp. 1-7.

[11] G. Mckee, P. Schenker, P., 1999, Sensor Fusion and Decentralized control in Robotic Systems II, SPIE Proceeding Series, Vol. 3839, pp. 270-278.

[12] L.W. Tsai, 1999, “Robot Analysis: The Mechanics of Serial and Parallel Manipulators”, John Wiley & Sons, Inc., pp. 116-164.

[13] L.W. Tsai, S. Joshi, 2002, “Kinematic Analysis of 3-DOF Position Mechanisms for Use in Hybrid Kinematic Machines”, Journal of Mechanical Design, Vol. 124, pp. 245–253.

[14] L.W. Tsai, 2000, Mechanism Design: Enumeration of Kinematic Structures According to Function, ISBN 0-8493-0901-8, CRC Press, Boca Raton, FL.

[15] A.K. Dash, I.M. Chen, S.H. Yeo, G.L. Yang, 2003, “Task-Based Configuration Design for 3-Legged Modular Parallel Robots Using Simplex Methods”, Proceedings 2003 IEEE International Symposium on Computational Intelligence in Robotics and Automation July 16-20, Kobe, Japan, pp. 998-1003.

[16] O. Ma, J. Angeles, 1991, “ Architecture Singularities of Platform Manipulators”, Proceeding of the 1991 IEEE International Conference on Robotics and Automation Sacramanto, California, April 1991, pp. 1542–1547.

[17] R.D. Gregorio, 2001, “Statics and Singularity Loci of the 3-UPU Wrist”, Proceedings of the 2001 IEEE/ASME International Conference on Advanced Intelligent Mechatronics, 8-12 July 2001, Como, Italy, pp. 470–475.